3th European Conference for Aero-space Sciences (EUCASS 2009)
July 6 – 9, 2009, Versailles, Paris

POSSIBILITIES OF RAREFIED GAS FLOW SIMULATION BY THE QUASI-GAS DYNAMIC EQUATION SYSTEM

Tatiana G. Elizarova and Jean-Claude Lengrand

Institute for Mathematical Modeling, Russian Academy of Sciences, Miusskaya pl. 4a, Moscow, 125047, Russia, telizar@yahoo.com, http://www.imamod.ru/∼elizar
CNRS/ICARE, 1C avenue de la recherche scientifique, 45071 Orléans Cedex 2, France

Abstract

The quasi-gas dynamic equation system that generalizes the Navier-Stokes equations is presented together with its kinetic origin. The advantages of this model for rarefied gas dynamic modeling are demonstrated in computations for microchannels, shock-wave structure, rarefied flows in underexpanded jets and in other flight physics problems.

Introduction

In the last years a number of attempts were undertaken to generalize the Navier-Stokes (NS) equations in order to extend their domain of validity when simulating moderately rarefied gas flows, see, e.g. [1] – [6]. But the constructed mathematical models are rather complicated, and far from practical applications. The quasi-gas dynamic (QGD) system, like the mentioned approaches, generalizing the possibilities of the NS system, can be regarded as a model with a non-classical continuity equation, but in contrast with the other models, the QGD system has been widely used for many years as an efficient computational tool.

The QGD algorithms have been implemented for 2D and 3D non-stationary viscous and inviscid flows, as well as for unstructured computational grids and parallel computing. The advantages of the QGD algorithms are found in the numerical modeling of rarefied gas flows, non-steady flows and fine grid implementations. Particulary, the QGD system allows extending the domain of validity of continuum equations in the direction of larger Knudsen numbers (Kn), compared with the NS system.

1. Regularized kinetic equation and construction of quasi-gas dynamic system

The QGD system was first obtained in 1982 based on a kinetic model consisting in a cyclic process of free-scattering – instantaneous maxwellization. The development of the QGD approach is reflected in Refs [7] – [18].

The regularized kinetic equation used to derive the QGD system can be obtained from the BGK equation

$$\frac{\partial f}{\partial t} + (\vec{\xi} \cdot \vec{\nabla}) f = \frac{f^{(0)} - f}{\tau}, \tag{1}$$

where the distribution function in the convective term is replaced by its approximation in the form of a Taylor expansion

$$f = f^{(0)} - \tau (\vec{\xi} \cdot \vec{\nabla}) f^{(0)}. \tag{2}$$

Here $f = f(\vec{x}, \vec{\xi}, t)$ is the one-particle distribution function, $f^{(0)}$ is the locally-equilibrium Maxwell distribution function, τ is the Maxwell relaxation time, that is close to the mean time between successive molecular collisions. This regularized equation writes

$$\frac{\partial f}{\partial t} + (\vec{\xi} \cdot \vec{\nabla}) f^{(0)} - (\vec{\xi} \cdot \vec{\nabla}) \tau (\vec{\xi} \cdot \vec{\nabla}) f^{(0)} = \frac{f^{(0)} - f}{\tau}. \tag{3}$$

In [8] was shown that for stationary flows if f satisfies Eq. (1), then it satisfies eq. (3) with the accuracy of $O(\tau^2)$ and vice-versa. The analog of the Boltzmann H-theorem was proved for eq. (3).

Averaging the model kinetic eq. (3) successively with the summation invariants 1, $\vec{\xi}$, $\xi^2/2$ we get the QGD system for a hard-sphere gas, with $\gamma = 5/3$, $Pr = 1$, and $p = \rho R T$.

According to [8], the obtained system can be presented under a conservative form as equations of continuity

$$\frac{\partial \rho}{\partial t} + \nabla_i J^i_m = 0, \tag{4}$$

conservation of momentum

$$\frac{\partial (\rho u^k)}{\partial t} + \nabla_i J^i_m u^k + \nabla^k p = \nabla_i \Pi^{ik}, \tag{5}$$

and conservation of total energy

$$\frac{\partial E}{\partial t} + \nabla_i \frac{J^i_m}{\rho} (E + p) + \nabla_i q^i = \nabla_i (\Pi^{ik} u^k), \tag{6}$$

where the mass flux vector J^i_m, the shear-stress tensor Π^{ik}, and the heat flux vector q^i are expressed as functions of macroscopic flow quantities in the following form

$$J^i_m = \rho u^i - \tau \left(\nabla_j (\rho u^i u^j) + \nabla^i p \right), \tag{7}$$

$$\Pi^{ik} = \Pi^{ik}_{NS} + \tau u^i \left(\rho u^j \nabla_j u^k + \nabla^k p \right) + \tau g^{ik} \left(u_j \nabla^j p + \gamma p \nabla_j u^j \right), \tag{8}$$

$$q^i = q^i_{NS} - \tau \rho u^i \left(u^j \nabla_j \varepsilon + p u_j \nabla^j (\frac{1}{\rho}) \right). \tag{9}$$

Here q^i_{NS} and Π^{ik}_{NS} are the Navier-Stokes heat flux and shear-stress tensor, while g^{ik} is the metric tensor.

In the above presentation we obtain that the viscosity coefficient μ, the bulk viscosity ζ and the heat conductivity κ are related through the parameter τ as

$$\mu = \tau p, \quad \zeta = \tau p \left(\frac{5}{3} - \gamma \right), \quad \kappa = \tau p \frac{\gamma R}{\gamma - 1}. \tag{10}$$

In this form the coefficients μ and κ were derived in constructing the NS system by the Chapman-Enskog method based on BGK model for the hard-sphere gas, see, for example [19]. The bulk viscosity coefficient ζ in the form (10) was obtained in [19] by the BGK approximation for polyatomic gas with rotational degrees of freedom.

As for the NS system obtained by the BGK approximation, the dissipative coefficients (10) can be generalized. Introducing a Prandtl number $Pr \neq 1$ we can write the coefficient of the heat conductivity in the usual form

$$\kappa = \mu \frac{\gamma R}{\gamma - 1} \frac{1}{Pr}.$$

Introducing the Schmidt number Sc (close to unity in gases) we obtain

$$\tau = \frac{\mu}{pSc}.$$

The bulk viscosity coefficient can also be generalized by introducing a numerical factor B to adjust it to a case of translational-rotational non-equilibrium

$$\zeta = \mu B \left(\frac{5}{3} - \gamma \right), \qquad \text{where} \qquad B = (\gamma - 1) \sqrt{\frac{\pi}{2}} \frac{3}{2} \sqrt{\frac{\pi}{8}} Z_{rot}, \tag{11}$$

and Z_{rot} is the coefficient of the energy exchange between translational and rotational degrees of freedom. The last one may be estimated by Parker's formula [20].

The QGD system is closely related to the NS system. For the QGD equations in the form (4) – (6), mass, momentum, angular momentum, total energy conservation laws, and the entropy theorem are valid as for the classic NS system.

Formally, QGD and NS systems differ from one another by terms contained τ that are of in the order of $O(\tau)$. But for stationary flows it was proved that these terms have the asymptotic order of $O(\tau^2)$ for $\tau \to 0$, or in the dimensionless form of the equations, of the order $O(Kn^2)$ for $Kn \to 0$. The boundary layer approximation for the QGD equations leads to the classical Prandtl equation system. The same approximation is valid for the NS system. From the definitions of the shear stress tensor (8) and heat flux vector (9) it follows that on the unpenetrated boundaries ($u^i = 0$) the shear-stresses and the heat fluxes for the QGD and NS models coincide, namely $\Pi = \Pi_{NS}$ and $q = q_{NS}$. So the definitions for the friction forces and the heat flux on the boundaries for the QGD and NS models are the same. The barometric Laplace formula is a common exact solution for both the QGD and NS models. Another exact solution for both models is the solution of the classical Couette problem [8].

The QGD system differs from the Burnett equations : the QGD system has additional terms in the form of second space derivatives, while the Burnett equations have additional third space derivative terms.

The QGD system can be regarded as an example of a model with non-classical continuity equation, or as a "two-velocities" gasdynamic model. The velocity u_i is related with the momentum transfer and frictions forces on the boundaries, while the J_m^i/ρ velocity describes the mass flow. One of the first variant of the "two-velocities" model was presented in 1951 [1]. Recently models of this type are widely proposed and investigated, e.g. [2] – [6]. Nevertheless, the QGD system differs significantly from the mentioned systems.

The advantages of the QGD model compared with the NS system are found for strongly non-stationary flows and for moderately rarefied flows, where terms contained τ are not negligible.

The QGD-algorithms are efficient in code implementation by virtue of the directly "built in" τ-regularization, ensuring a high quality of the numerical solution. Finite-difference approximations are constructed by the control volume method in a flux form, corresponding to conservation laws. All gas dynamic parameters are determined in the nodes of the computational grid. The central difference approximation for all space derivatives, including the convective terms, is used. For efficient simulations of flows with moderate and small Kn the parameter τ can be taken in the form $\tau \sim (\lambda/c) + (h/c)$, where h is the mean size of the computational grid.

3. Rarefied flow simulations

Microchannel flows. Experiments of Knudsen, carried out in 1900, show the existence of a minimum in the normalized flow-rate in long isothermal microchannels for $Kn \sim 1$. The possibilities of describing this phenomenon is a present-day problem for rarefied flow simulations in the framework of continuum models. The NS equation system with Maxwell-type slip boundary conditions fails to describe this effect. Using the NS system the Knudsen effect may be obtained by introducing artificial second order slip boundary conditions, e.g. [21]. Some results were obtained, for example, by 13-moment regularized Grad equations by a rather difficult mathematical technique together with enhanced boundary conditions [22]. Based on the BGK model for hard-sphere molecules the Knudsen effect has been described by a complex mathematical procedure in [23].

The QGD system complemented by the classical Maxwell-type slip boundary conditions allows to obtain the mass flow-rate formula describing the Knudsen effect in a simple way.

We analyze a gas flow in a plane channel of length L in x–direction and depth H in y–direction. The pressures at entrance and exit of a channel are p_1 and p_2, respectively, where $p_1 > p_2$. We look for the solution of the system (4)–(6) in the form $u_x = u(y)$, $u_y = 0$, $p = p(x)$, $T = T_0$. In this case the NS and QGD systems reduce to the same equation

$$\frac{dp(x)}{dx} = \mu \frac{d^2u(y)}{dy^2}.$$

Using Maxwell velocity-slip boundary condition in the form

$$u_s = \frac{2-\sigma}{\sigma}\lambda\frac{\partial u}{\partial y}$$

for both systems we get the classical modified Poiseuille formula for the velocity distribution

$$u_x(y) = -\frac{1}{2\mu}\frac{dp(x)}{dx}\Big[y(H-y) + \frac{2-\sigma}{\sigma}\lambda H\Big].$$

Here σ is the coefficient of accommodation for velocity, and λ is the mean free path calculated as $\lambda = A\mu\sqrt{RT}/p$, where, e.g., $A = \sqrt{\pi/2}$ for a hard-sphere gas (Chapman), or $A = 2(7-2\omega)(5-2\omega)/(15\sqrt{2\pi})$ for a VHS gas (Bird, [20]).

In the QGD formulation the flow-rate is calculated using the mass flux (7) $J_{mx} = \rho(u_x - w_x)$, as

$$J = \int_0^H J_{mx} dy, \quad \text{where} \quad w_x = -\frac{\tau}{\rho}\frac{dp}{dx} = -\frac{\mu}{pSc}\frac{1}{\rho}\frac{dp}{dx}.$$

So the normalized flow-rate becomes

$$Q_{xy} = \frac{J}{J_0^{xy}} = \frac{3\sqrt{\pi}A}{8\sqrt{2}}\Big[\frac{Kn^{-1}}{6} + \frac{2-\sigma}{\sigma} + \frac{2}{A^2\,Sc}Kn\Big]. \tag{12}$$

The first term in (12) describes the mass flow-rate for non-slip Poiseuille flow, the second one accounts for the flow-rate increase because of velocity-slip conditions, the third one explains the flow-rate increase because of self-diffusion. It does not depend on σ. This last term has the order of $O(\tau \cdot \mu)$ or $O(Kn^2)$, where $Kn = \lambda/H$. For stationary flows this fact corresponds to the difference between QGD and NS models in stationary cases. The importance of the self-diffusion for rarefied flows in microchannels is pointed out in, e.g. [23]. The minimum of Q_{xy} takes place for

$$Kn_m = \frac{A}{2}\sqrt{\frac{Sc}{3}}.$$

This value does not depend on σ. For $Sc = 1$, $A = \sqrt{\pi/2}$, $Kn_m = 0.36$. The results obtained together with the results e.g. [9], [10], [18] show, that for this problem the QGD model increases the domain of validity of the continuum approach up to $Kn \sim 0.5$.

Shock-wave problem. The shock-wave problem is a widely used test for mathematical models and numerical algorithms in rarefied flow simulations.

Below we compare the structure of shock wave fronts at different Mach numbers (Ma), modeled via NS and QGD equations, with experimental results from the literature. Monoatomic argon, and diatomic nitrogen, are considered. The molecular parameters are taken from [20]. In this modeling a finite-difference scheme with second-order spatial accuracy is employed for both the NS and QGD equations [9], [16].

In Fig. 1, left, the distributions of velocity, density and temperature in an argon shock wave are shown together with experimental data. The density thickness calculated via QGD and NS models ($\gamma = 5/3, \omega = 0.81, Sc = 0.752, Pr = 2/3$) are in a good agreement with each other, and with the experimental results. But velocity and temperature profiles in the upstream region differ. In the QGD formulation they are smoothed compared with the NS one. This effect is similar to that found for BGK modeling. The QGD-based algorithm converges to the steady state solution approximately 10 times faster than the NS-based algorithm due to the absence of numerical oscillations (Fig. 1, right). The values of the reciprocal shock-wave thickness for QGD and NS calculations are close one to each other, and both differ from the experiment by $\sim 30\%$ for $Ma > 2$.

Calculations for diatomic nitrogen in the NS and QGD formulations ($\gamma = 7/5, \omega = 0.74, Sc = 0.746, Pr = 14/19$) were performed taking into account the bulk viscosity in the form (11). Here again the QGD results for the density distributions are close to the NS ones.

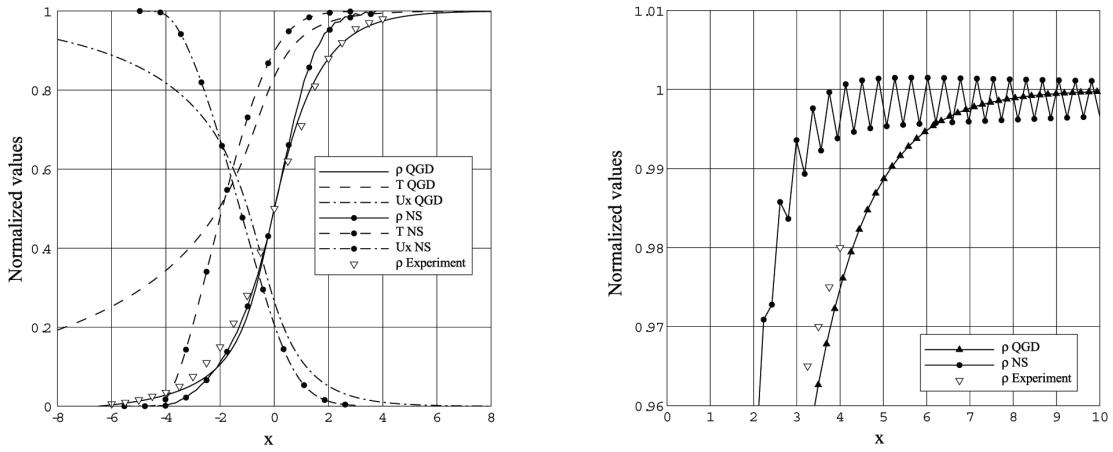

Figure 1: Density, velocity and temperature distributions in argon shock-wave, $Ma = 9$ (left). Fragment for the density distribution (right) Comparison of the QGD and NS solutions with the experiment.

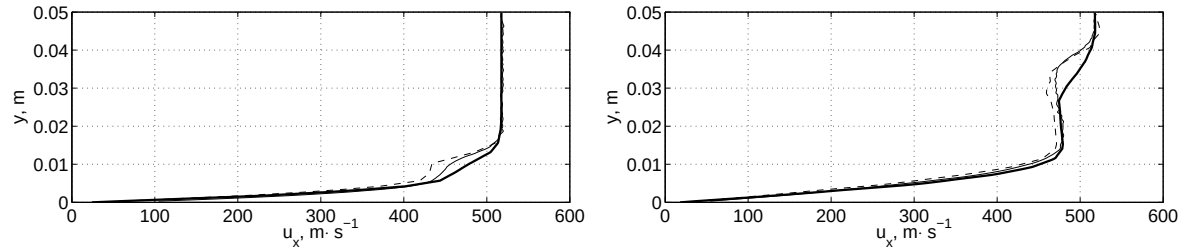

Figure 2: Longitudinal velocity profiles for the flow along a flat plate at a distance from leading edge $x = 4$ cm (left) and 7 cm (right). DSMC - solid line, QGD - bold solid line, NS - dashed lines.

Both depend strongly on the value of the bulk viscosity. If the numerical factor B in (11) is taken according to translational-rotational exchange law, the calculated shock-wave densities differ moderately from experimental data even for $Ma > 2$.

Flat-plat flow. The comparison of the QGD, NS and Direct Monte Carlo (DSMC) calculations for the supersonic air flow near a flat plate is shown in Fig. 2. Parameters of the undisturbed flow are: $Ma = 2$, $\rho = 0.000169\,\text{kg/m}^3$, $T = 167$ K, $u = 518$ m/s. The surface temperature is $T_w = 300K$, the length of the plate is 12 cm. Slip velocity and temperature-jump conditions are imposed on the surface [17].

In this flow $Kn \sim 0.01$, and as it is seen from Fig. 2, the velocity profiles calculated by DSMC (reference data), NS and QGD systems, are extremely close one to one another. The DSMC velocity distributions are always placed between the NS and the QGD lines. Comparison of the convergence rate shows that the computational time for the QGD algorithm is less than the NS computational time by a factor of 20. The difference arises from the smaller NS computational time step and the greater number of time steps required to achieve convergence.

Rarefied interacting plumes. Experimental and numerical investigations of the interaction of two rarefied underexpanded parallel plumes and of the interaction of a plume with a par-

allel plate were performed. In the experimental setup nitrogen jets were issued from one or two parallel conical nozzle(s) that simulated satellite control thrusters. The twin plumes (type I) were issued from 15-degrees half-angle conical nozzles with critical radii $r_c = 0.2$ mm, stagnation conditions $T_0 = 900$ K and $p_0 = 12$ bars. The single plume (type X) was issued from a 7-degrees half-angle conical nozzle with the same critical radii, stagnation conditions $T_0 = 1100$ K and $p_0 = 16$ bars. The distance between the parallel axes of jets I was 50 mm and the distance between the axis of jet X and the flat plate, parallel to it, was 17 mm. Experimental investigations consisted in determining flowfield density by means of electron beam surveys and measuring wall pressure.

Flow conditions and gas parameters corresponding to the experimental results are given in Table 1 for two variants of jets, namely jet X and jet I. Subscript $_e$ corresponds to the conditions at nozzle exit, $_\infty$ corresponds to the background gas, $_w$ refers to wall conditions. Here r_e denotes the nozzle exit radius, λ - the mean free path. The Knudsen number Kn_e is defined as $Kn_e = \lambda_e/(2r_e)$. Other data are $\gamma = 1.4$, $Pr = 14/19$, $T_\infty = T_w = 293$ K, $p_\infty = 1$ Pa.

Table 1: Flow parameters

	Jet I	Jet X
r_e (m)	$1.6 \cdot 10^{-3}$	$1.7 \cdot 10^{-3}$
λ_e (m)	$1.304 \cdot 10^{-6}$	$1.397 \cdot 10^{-6}$
Kn_e	$4.07 \cdot 10^{-4}$	$4.1 \cdot 10^{-4}$
Ma_e	5.781	5.813
T_e (K)	117.1	141.8
p_e (Pa)	954	1230
u_e (m/s)	1275	1411

Fig. 3 represents the calculated and measured number density contours in the (x, z) symmetry plane ($y = 0$). The actual computational domain took advantage of the symmetry plane(s) in the configurations investigated. On the figures the computational domain was doubled according to the symmetry plane conditions. In the present numerical results, the interaction between the jets begins at a distance x somewhat smaller than in the experiment. Except for this small difference, the calculated contours match well the experimental ones [15].

Orbiter flow simulations. This work was related to the aerocapture phase of the Mars Sample Return (MSR) mission, as it was planned jointly by CNES and NASA. During the aerocapture, the vehicle passes through the Martian atmosphere, which decreases its velocity and allows it to orbit the planet. Its altitude first decreases, changing the flow regime from free molecular (FM) to continuum. Then the altitude increases again, changing the regime back to FM. A typical trajectory was retained, where the Mach number varies from 18 up to 30 and the Knudsen number from 10^{-4} to 0.2. Based on classical criteria, the continuum flow regime holds from $t = 90$ s to $t = 210$ s and the FM regime holds for $t \geq 540$ s. Different methods, appropriate to the different regimes have been used to predict a number of quantities of interest, including the heat transfer q at the stagnation point. The flow was calculated around a simplified MSR orbiter, around an infinitely thin disk oriented perpendicular to the free stream and around a bluff-faced cylinder with diameters of the disk and of the cylinder equal to that of the orbiter.

The influence of numerical and physical parameters was studied first under the hypotheses of a pure-CO2 atmosphere, considering a perfect diatomic gas [14]. In Fig. 4 the trajectory parameters and the calculated stagnation point heat transfer rate have been plotted for different methods. If DSMC is considered as a reference, the results demonstrate that the continuum approaches (QGD equations and integral method) as well as the free-molecular estimates can be used well inside the transition regime.

The QGD system was successfully used in other numerical simulations of rarefied gas flows, e.g. underexpanded jets [11], supersonic flows around an infinitely thin disk [13] and others. The possibilities of extending the QGD model to thermal non-equilibrium flows and to binary gas mixtures are presented, e.g., in [9] and [12].

Conclusion

The quasi-gasdynamic equation system that generalizes the Navier-Stokes equations has been presented together with its kinetic origin. The advantages of this model in rarefied gas dynamics are demonstrated for microchannels, shock-wave structure and flow computations, that

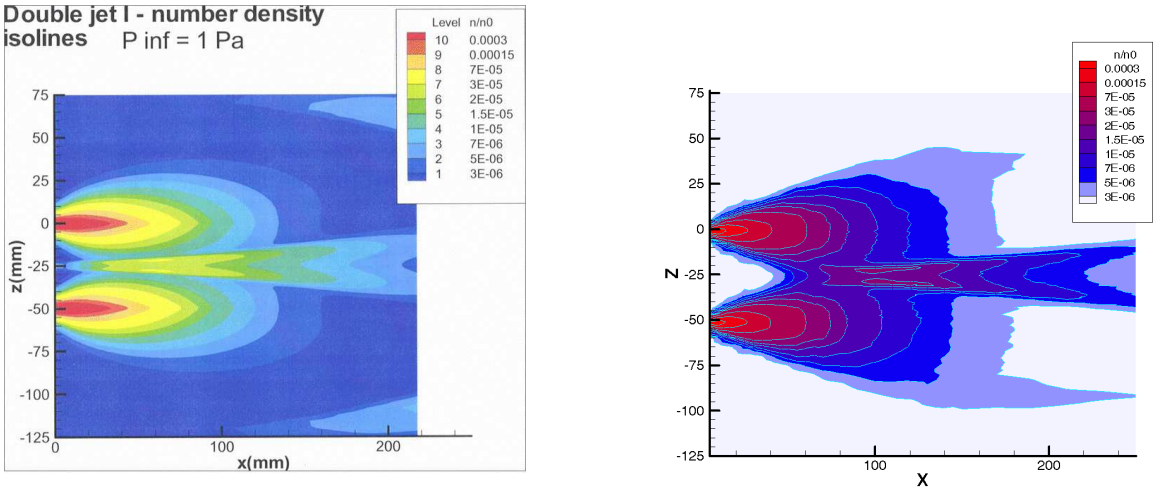

Figure 3: Calculated (left) and measured (right) density contours for the double jet I

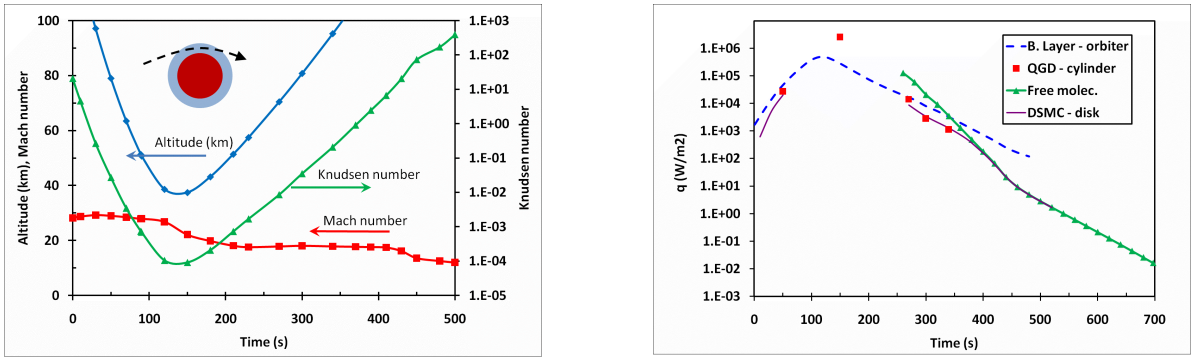

Figure 4: Trajectory parameters (left) and heat transfer rate at stagnation point vs. time (right)

include a wide range of rarefaction parameters.

Theoretical investigations and numerical experience show, that for rarefied gas flows up to $Kn \sim 0.1$ the QGD and NS results coincide. For practical applications the form of quasi-gas dynamic equations allows to use a uniform and robust numerical algorithm and may be competitive with the modern Navier-Stokes based methods. For rarefied flows up to $Kn \sim 0.5$ the QGD results correspond better with the experiment data than the NS results if the same Maxwell-type boundary conditions are used.

References

[1] S.V. Vallander: Equations of motion for viscous gas, *Dokl. of USSR Ac. of Science*, 58, pp.25–27 (1951).

[2] B.V. Alexeev, *Generalized Boltzmann physical kinetics*, Elsevier, Amsterdam (2004).

[3] Yu.L. Klimontovich: About the necessity and possibility of unified description of kinetic and hydrodynamic processes, *Theoretical and Mathematical Physics*, Vol. 92, pp. 312–330 (1992).

[4] H. Brenner, Fluid Mechanics Revisited, *Physica A*, 370, pp.190–224 (2006).

[5] H.C. Ottinger: *Beyond equilibrium thermodynamics*, Hoboken, John Wiley, (2005).

[6] R.F. Streater: The dissipative continuity equation, *17 th International Conference on Transport Theory*, Imperial College, 8– 14 July, 2001.

[7] B.N. Chetverushkin: *Kinetically-consistent finite-difference schemes in gasdynamics*, Moscow, MGU, (1999) (in Russian).

[8] Yu.V. Sheretov: *Mathematical modeling of liquid and gas flows based on quasi-hydrodynamic and quasi-gasdynamic equations*, Tver State university, Tver, (2000) (in Russian).

[9] T.G. Elizarova: *Quasi-gasdynamic equations and numerical methods for viscous flow computations*, Scientific world, Moscow, (2007) (in Russian). English translation by Springer (2009).

[10] T.G. Elizarova, Yu.V. Sheretov: Analyse du problème de l'écoulement gazeux dans les microcanaux par les équations quasi hydrodynamiques, *La Houille Blanche. Revue Internationale de l'Eau*, No 5, pp. 66–72 (2003).

[11] I.A. Graur, T.G. Elizarova, A. Ramos, G. Tejeda, J.M. Fernandez, S. Montero: A study of shock waves in expanding flows on the basis of spectroscopic experiments and quasi-gasdynamic equations. *Journal of Fluid Mechanics*, Vol.504, pp. 239–270 (2004).

[12] T.G. Elizarova, I.A. Graur, J.C. Lengrand: Two-fluid computational model for a binary gas mixture.*European Journal pf Mechanics (B/Fluids)*, Vol. 3, pp. 351–369 (2001).

[13] A. Chpoun, T.G. Elizarova, I.A. Graur, J.C. Lengrand: Simulation of the rarefied gas flow around a perpendicular disk, *European Journal of Mechanics (B/ Fluids)*, Vol 24, pp.457 –467 (2005).

[14] E. Chabut,J.C. Lengrand, T.G. Elizarova, M.E. Sokolova: A comparison of different numerical approaches for calculating a Martian entry flow. *European Conference for Aerospace science (EUCASS)*, Moscow, July 2005.

[15] I.A. Chirokov, T.G. Elizarova, J.C. Lengrand, I.A. Graur, I. Gibek: Experimental and numerical investigation of rarefied interacting plumes, *Proc. of the 23th Intern. Symp.on Rarefied Gas Dynamics*, edited by A.D. Ketsdever and E.P.Muntz, American Institute of Physics, Whistler, Canada, pp.572–579 (2003).

[16] I.A. Shirokov, T.G. Elizarova, S. Montero: Numerical simulation of shock-wave structure in argon, helium and nitrogen, Proc. of the 24-rd International Symposium on Rarefied Gas Dynamics, edited by M. Capitelli, AIP Conference Proceedings Vol.762, pp.1253–1258 (2005).

[17] A.A. Khokhlov: *Navier-Stokes equations and their modifications for gas flow simulations*, Ph.D. thesis, Moscow State University, Physical faculty, (2007) (in Russian).

[18] T.G. Elizarova: Knudsen effect and a unified formula for mass flow-rate in microchannels, *Proc. of the 25th international symposium on rarefied gas dynamics*, edited by M.S. Ivanov and A.K. Rebrov, Siberian Branch of RAS, Novosibirsk, pp.1164–1169 (2007).

[19] W.G. Vincenti, Jr.C.H. Kruger: *Introduction to Physical Gas Dynamics*, Wiley, (1965).

[20] G.A. Bird: *Molecular gas dynamics and the direct simulation of gas flows*, Clarendon press, Oxford, (1998).

[21] G. E. Karniadakis, A. Beskok, N. Aluru: *Micro Flows: Fundamentals and simulation*, Springer, Berlin, (2005).

[22] X.J. Gu, D.R. Emerson: A computational strategy for the regularized 13 moment equations with enhanced wall-boundary conditions, *Journal of computational physics*, 225, pp.263–283 (2007).

[23] C. Cercignani, *Theory and application of the Boltzmann equation*, Scottish Academic Press, London, (1975).